http://dx.doi.org/10.5012/bkcs.2011.32.12.4205

Structural and Electrochemical Properties of $Li_2Mn_{0.5}Fe_{0.5}SiO_4/C$ Cathode Nanocomposite

Youngmin Chung, Seungho Yu, Min Seob Song, Sung-Soo Kim,[†,*] and Won Il Cho[*]

Energy Storage Research Center, Korea Institute of Science and Technology, Seoul 136-791, Korea. [*]E-mail: wonic@kist.re.kr
[†]Graduate School of Green Energy Technology, Chungnam National University, Deajeon 305-764, Korea
[*]E-mail: kimss@cnu.ac.kr
Received August 9, 2011, Accepted October 1, 2011

The $Li_2Mn_{0.5}Fe_{0.5}SiO_4$ silicate was prepared by blending of Li_2MnSiO_4 and Li_2FeSiO_4 precursors with same molar ratio. The one of the silicates of Li_2MnSiO_4 is known as high capacitive up to ~330 mAh/g due to 2 mole electron exchange, and the other of Li_2FeSiO_4 has identical structure with Li_2MnSiO_4 and shows stable cycle with less capacity of ~170 mAh/g. The major drawback of silicate family is low electronic conductivity (3 orders of magnitude lower than $LiFePO_4$). To overcome this disadvantage, carbon composite of the silicate compound was prepared by sucrose mixing with silicate precursors and heat-treated in reducing atmosphere. The crystal structure and physical morphology of $Li_2Mn_{0.5}Fe_{0.5}SiO_4$ was investigated by X-ray diffraction, scanning electron microscopy, and high resolution transmission electron microscopy. The $Li_2Mn_{0.5}Fe_{0.5}SiO_4$ / C nanocomposite has a maximum discharge capacity of 200 mAh/g, and 63% of its discharge capacity is retained after the tenth cycles. We have realized that more than 1 mole of electrons are exchanged in $Li_2Mn_{0.5}Fe_{0.5}SiO_4$. We have observed that $Li_2Mn_{0.5}Fe_{0.5}SiO_4$ is unstable structure upon first delithiation with structural collapse. High temperature cell performance result shows high capacity of discharge capacity (244 mAh/g) but it had poor capacity retention (50%) due to the accelerated structural degradation and related reaction.

Key Words : Lithium manganese iron silicate, Polyanion system, Cathode, Physical blending, Lithium-ion battery

Introduction

Rechargeable lithium-ion batteries are becoming increasingly important as power sources for portable electronics and large-scale applications they are being intensively pursued for vehicle applications including hybrid electric vehicles (HEV), plug-in hybrid electric vehicles (PHEV), and electric vehicles (EV). However, the major challenge including safety, toxicity, and cost of these materials inhibit their further use in price sensitive and large-scale applications.

Most common in Li-ion battery cathode materials, such as $LiCoO_2$, $Li[Ni, Mn, Co]O_2$, and $LiMn_2O_4$, show various characteristics of merits and drawbacks in standpoint of resource scarcity, energy density and safety etc. Concerning of safety introduced cathodes containing polyanions such as XO_4^{2-} and the discovery of electrochemical properties of $LiFePO_4$ have given significant impacts. The structural stability afforded by strong covalent P-O bond, gives considerable safety enhancement. Further step in search for stabilized structures seem to be replacement phosphorous with silicon. Recently, two materials from a new family of transition metal silicate, namely Li_2MnSiO_4 and Li_2FeSiO_4 have been successfully prepared and preliminary tested for positive electrode materials.[1-5] Although the primary motivation for preparing the silicate system was safety (thermal stability), it was hoped that at least the Li_2MnSiO_4 analogue could open exciting new prospects in the search for high-capacity cathode materials. Polyanion - containing framework that can reversibly insert/extract two lithium ions per formula unit would help to increase the capacity and energy density while benefiting from the highly stable covalently bonded XO_4 groups.

The major drawbacks of the silicate family are their characteristically low electronic conductivity, which has been shown to be up to 3 orders of magnitude lower than that of $LiFePO_4$ [6] and obtaining a phase-pure material by many methods is a challenge, as most of the synthesis method produce impurities such as Li_2SiO_3, Fe_3O_4, and Mn_2SiO_4, resulting in low capacities.[7,8] Li_2MnSiO_4 is inherently unstable and tend to collapse, and with a reduction in particle size and coating with conductive carbon, capacities close to 200 mAh/g have been recently. Atomistic simulations further show that mixing with Li_2FeSiO_4 could yield the optimal compromise between structural stability and high utilization. Kokalj analyzes experimentally and by simulations based on density functional theory[9] which suggests $Li_2Mn_{0.5}Fe_{0.5}SiO_4$ system could suitable for $Li_2Mn_xFe_{1-x}SiO_4$ system.

$Li_2Mn_{0.5}Fe_{0.5}SiO_4$ material could give structure stability since suitable sequential energy cost and unit cell volume change while charge/discharge. However, synthesizing $Li_2Mn_{0.5}Fe_{0.5}SiO_4$ is difficult since Mn and Fe-ion were existed in the same solution condition, Mn-ion could make fast reaction than Fe-ion. Mn-ion's reactivity is high that means

Fe-ion is stable and inactive in the same solution synthesis condition. In the sol-gel solution could not give perfect synthesis condition for $Li_2Mn_{0.5}Fe_{0.5}SiO_4$, therefore we have tried to synthesize for $Li_2Mn_{0.5}Fe_{0.5}SiO_4$ through blending of Li_2MnSiO_4 and Li_2FeSiO_4 precursors, each Li_2MnSiO_4 and Li_2FeSiO_4 precursors was separately prepared by suitable method.

In this paper, simply precursors blending method is used to synthesize $Li_2Mn_{0.5}Fe_{0.5}SiO_4$. With aim to synthesizing obtain Mn and Fe mixed in silicate system and characterization of carbon-decorated $Li_2Mn_{0.5}Fe_{0.5}SiO_4$/C nanocomposite material and investigate effect of cycling ability by extract-insertion of changing Lithium-ion amount.

Experimental

Synthesis of Li_2MnSiO_4 and Li_2FeSiO_4 Precursor. All of synthesis process of the $Li_2Mn_{0.5}Fe_{0.5}SiO_4$/C nanocomposite indicates in the Figure 1. Li_2MnSiO_4 and Li_2FeSiO_4 precursor synthesized separately by sol-gel and ball mill process respectively. For the synthesis of Li_2MnSiO_4 precursor, stoichiometric amount of lithium acetate (Sigma Aldrich 99+%), manganese acetate (Aldrich 99+%), and Tetraethyl orthosilicate (Aldrich reagent grade 98%) were dissolved in ethanol under magnetic stirring at 80 °C for 24 h. The solution was dried at 80 °C over night. The obtained dry gel was grounded. For the synthesis of Li_2FeSiO_4 precursor, stoichiometric amount of lithium acetate, Ferric citrate (Aldrich 99+%), and Tetraethyl orthosilicate were dissolved in ethanol was mixed for 10 h by a planetary mill (Fritsch Pulverisette 5). The milling speed was 300 rpm. The ball milled solution was dried at 80 °C over night. The obtained dry gel was grounded.

Synthesis of $Li_2Mn_{0.5}Fe_{0.5}SiO_4$ Nanocomposite. Prepared Li_2MnSiO_4 and Li_2FeSiO_4 precursors were also mixed by planetary mill (Fritsch Pulverisette 5). For the synthesis stoichiometric amount of each precursors and 9 wt % of sucrose (Aldrich 99+%) added to acetone. Then, these were mixed for 2 h, 300 rpm by a planetary mill. This milled solution was dried at 80 °C for 4 h and sintered at 600 °C for 10 h in flowing N_2+ 10% H_2 Mixed gas.

Structural and Chemical Characterization. Powder X-ray diffraction (XRD; Rigaku D/max-II A) employing was used to identify the crystalline phase of prepared powder and filtered Cu Kα radiation between 10°-90°(2θ). The morphology was observed with a scanning electron microscope (SEM: Nova nanoSEM200) and high resolution transmission electron microscopy (HR-TEM: Tecnai G2) and energy dispersive spectroscopic (EDS).

Electrochemical Characterization. Electrochemical performances were evaluated with CR2032 type coin cells. Lithium metal foils were used as anode and Celgard 2500 film as a separator. The cathode electrodes were fabricated from a mixture of active material, acetylene black (Denka black), polyvinylidene fluoride (PVDF) in a weight ratio of 85:10:5. *N*-Methyl pyrrolidone (NMP) was used to make slurry of the mixture. After homogenization, the slurry was coated on an aluminum foil and dried at 80 °C for 12 h. The electrode was then roll-pressed and disks were punched out. Cells were assembled in a dry room. The electrolyte solution was 1 M $LiPF_6$ in a mixture ethylene carbonate (EC), dimethyl carbonate (DMC), ethylmethyl carbonate (EMC) (1:1:1 volume ratio). The cells were examined by using a battery testing system (Maccor 4000) at a current density of 0.05 C between 2.0-4.8 V 10 cycles. Cyclic voltammetry was conducted (CV, Biology SAS) with a voltage range of 2.0-4.5 V at 0.1 mV/sec. High temperature cell performance were also examined at 0.05 C between 2.0-4.5 V 10 cycles at 55 °C.

Results and Discussion

Structural and Chemical Characterization. Figure 2 shows the XRD pattern of the carbon-coated $Li_2Mn_{0.5}Fe_{0.5}SiO_4$/C. Sample powder can be indexed on the basis orthorhombic unit cell with the space group $Pmn2_1$, which is proposed to be iso-structural with low-temperature β-Li_3PO_4.[2] However, it is apparent that the peaks are not defined clearly, indicating low crystalline properties of synthesized Li_2MSiO_4. That could be attributed to the high energy milling process, low heat-treatment temperature and variety of polymorphs. Li_2MSiO_4 materials were known to crystal-

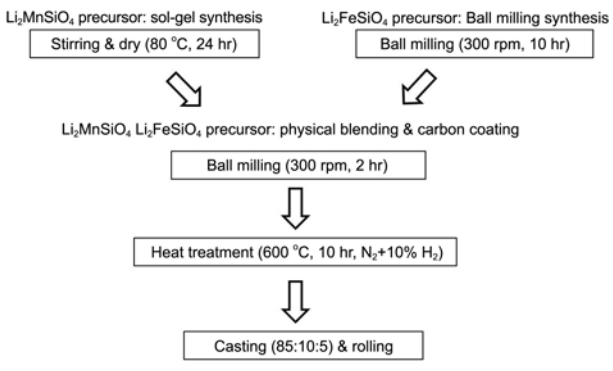

Figure 1. Synthesis process of the $Li_2Mn_{0.5}Fe_{0.5}SiO_4$/C nanocomposite.

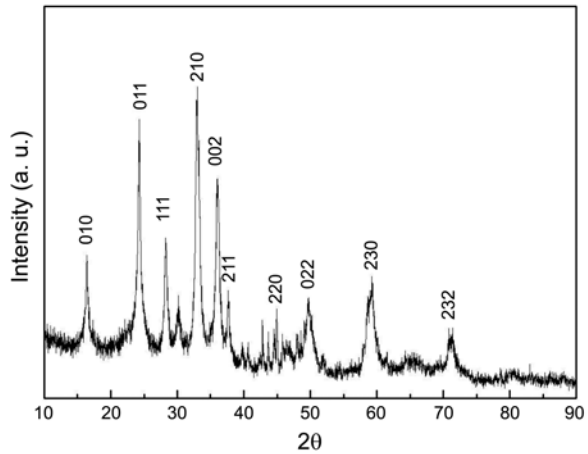

Figure 2. XRD pattern of $Li_2Mn_{0.5}Fe_{0.5}SiO_4$/C sample.

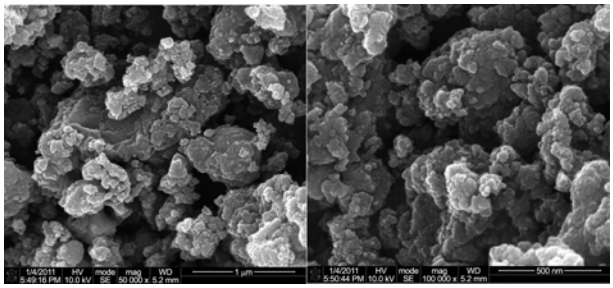

Figure 3. SEM image of $Li_2Mn_{0.5}Fe_{0.5}SiO_4$/C nanocomposite.

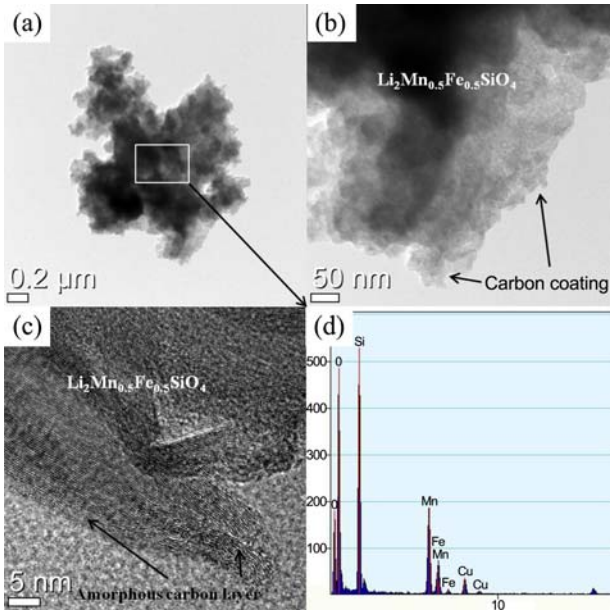

Figure 4. (a) TEM image of $Li_2Mn_{0.5}Fe_{0.5}SiO_4$/C nanocomposite, (b), (c) HR-TEM indicates the presence of carbon layer, and (d) EDS analysis of the corresponding sample.

lize in various polymorphs, depending on the synthesis conditions employed.[7,10] Crystal imperfections such as stress, deformation, twinning and composition inhomogeneity can also contribute to the peak broadening. Proposed a β-Li_3PO_4 -based structure with *Pmn*2_1 symmetry for Li_2FeSiO_4, where the lithium ions occupy the tetrahedral sites in between the layers comprising chains of alternating pairs of FeO_4 and SiO_4 tetrahedral running along with the α direction. It is known that the Li_2FeSiO_4 and Li_2MnSiO_4 is iso-structural with close lattice parameters and it is easy to form solid solution of $Li_2Mn_xFe_{1-x}SiO_4$.[13] However, recent high resolution X-ray diffraction and transmission electron microscopy studies have revealed that the structure can be better refined with a $P2_1$ monoclinic with alternating pairs of FeO_4 and SiO_4 tetrahedral.[11] Crystal imperfections such as stress, deformation, twinning and composition inhomogeneity can also contribute to the peak broadening. The XRD peaks due to carbon do not show that attributed to its amorphous nature and content. Elemental analysis of heat treated $Li_2Mn_{0.5}Fe_{0.5}SiO_4$ samples by ICP gave a Li/Mn + Fe ratio of 2:1, confirming the stoichiometry.

The particle morphology of $Li_2Mn_{0.5}Fe_{0.5}SiO_4$/C nanocomposite was observed by SEM (Figure 3) and HR-TEM (Figure 4). Nanoparticles can be observed in both images and attributed to the homogeneity of the Li_2MnSiO_4 and Li_2FeSiO_4 precursor. Figure 3 exhibits nanocomposite morphology with a particle diameter of approximately ~300 nm that is a result of an agglomeration of the nanoparticles with an average size of 30 nm which nanocomposite morphology is beneficial for increasing the tap density, as the larger size of the secondary particles (~300 nm) allows for a denser packing, while the smaller size of the primary particle (~30 nm) improves the lithium-ion and electron conduction.[12]

The HR-TEM images in (Figure 4) show amorphous carbon coating on the $Li_2Mn_{0.5}Fe_{0.5}SiO_4$/C nanocomposite. The images clearly indicate the appearance of weakly aggregated nano particulates with sizes less than 50 nm. Figure 4(c) confirmed the presence of almost homogeneous carbon layer on the $Li_2Mn_{0.5}Fe_{0.5}SiO_4$/C. HR-TEM EDS analysis (Figure 4(d)) was also conducted to examine the chemical composition of $Li_2Mn_{0.5}Fe_{0.5}SiO_4$/C which indicates presence of Mn, Fe, Si, and O. According to EDS results, the atomic ratio of Mn and Fe is not exactly same, but it might be considered within the limit of allowable error range. This result of TEM reveals that precursor blending process prevents particles growth at solution phase reaction effectively. Thereafter, during high temperature sintering at inert atmosphere, the sucrose was carbonized and form as carbon on the surface, which prevents the growth of particles as well as enhances the electronic conductivity of the material. The small particle size of Li_2MSiO_4 provides short path ways for rapid lithium-ion and electron conduction within the nanoparticles, while the carbon coating connects the nanoparticles in close proximity, providing a highly conductive channel for the electron mobility between adjacent Li_2MSiO_4 nanoparticles.

Electrochemical Characterization. The silicate Li_2MnSiO_4 structure has become appealing, as it could theoretically insert/extract two lithium per formula unit with a theoretically capacity of ~330 mAh/g[2] and the strong bond of Si-O polyanion could stabilize and give advantage in aspect of cell safety like $LiFePO_4$. Following this silicate with the general formula Li_2MSiO_4 (M=Mn, Fe and Co) have been identified as potential lithium insertion/extraction hosts.[10-13] Among them, Li_2FeSiO_4 has drawn the attention, exhibiting a stable cycle life with a reversible practical capacity around 160 mAh/g.[7,11] Li_2FeSiO_4 would be converted to $LiFeSiO_4$, the potential plateau are flat and stable around 2.8 V, represents the oxidation of Fe^{2+} to Fe^{3+}, except 1st charging at 3.1 V, due to the irreversible structural rearrangement.[15]

Li_2MnSiO_4 has two redox couples ($Mn^{2+/3+}$ and $Mn^{3+/4+}$), whereas Li_2FeSiO_4 only has one redox couple ($Fe^{2+/3+}$). Therefore two electrons are expected to be involved in the deintercalation-intercalation process of Li_2MnSiO_4, and the theoretical capacity of Li_2MnSiO_4 is twice as high as that of Li_2FeSiO_4.[14]

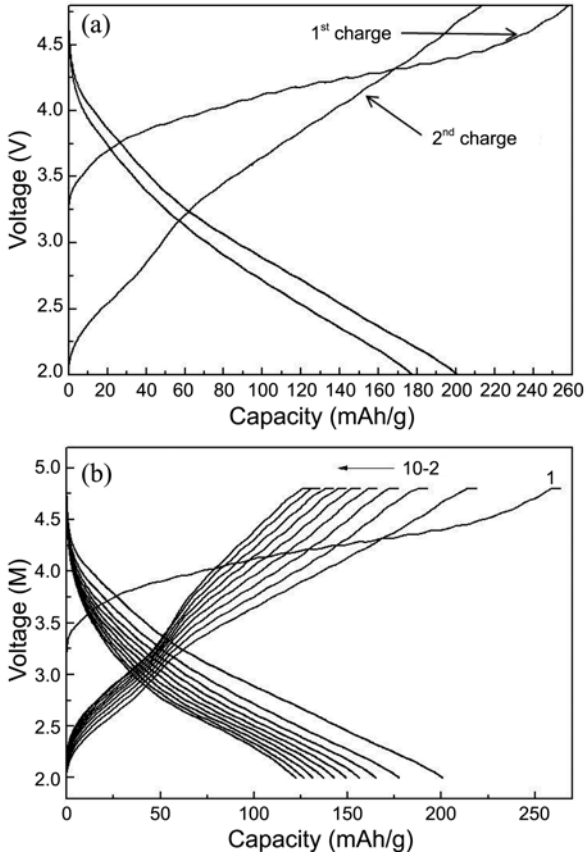

Figure 5. First and second charge-discharge profile recorded and cycling performance at C/20 rate room temperature. (a) charge-discharge curve of $Li_2Mn_{0.5}Fe_{0.5}SiO_4$/C, (b) cycling performance of $Li_2Mn_{0.5}Fe_{0.5}SiO_4$/C.

Galvanostatic charge-discharge measurements were carried out with lithium cells at 0.05 C rate to evaluate the electrochemical properties of $Li_2Mn_{0.5}Fe_{0.5}SiO_4$/C nanocomposite cathode at room temperature. Figure 5(a) shows the first and second charge-discharge profiles and Figure 5(b) shows cycling performance during 10 cycles of the $Li_2Mn_{0.5}Fe_{0.5}SiO_4$/C nanocomposite in the potential range of 2.0-4.8 V. The $Li_2Mn_{0.5}Fe_{0.5}SiO_4$/C nanocomposite delivers a first discharge capacity of 200 mAh/g. As seen in Figure 5(a), second charge curve is different from the first charge profile, however $Li_2Mn_{0.5}Fe_{0.5}SiO_4$/C nanocomposite shows (Figure 5(b)) monotonous voltage profile subsequent cycles. The Similar phenomenon was reported as the structure rearrangements involving the exchange of lithium, manganese, and iron between their sites during first charge in crystalline Li_2FeSiO_4, as indicated by XRD measurement.[15] In this $Li_2Mn_{0.5}Fe_{0.5}SiO_4$/C nanocomposite, the voltage profile change between 1st and 2nd cycle comes from drastic structural deformation like amorphization, rather than rearrangement. It is known that close to 1 mole lithium per formula can be extracted/inserted from/into Li_2FeSiO_4/C, more than 1 lithium ion per formula can be extracted/inserted from/into Li_2MnSiO_4/C. The initial capacity more than 200 mAh/g means that the reaction amounts is more than 1 mole lithium per formula. Additionally, higher charge potential was

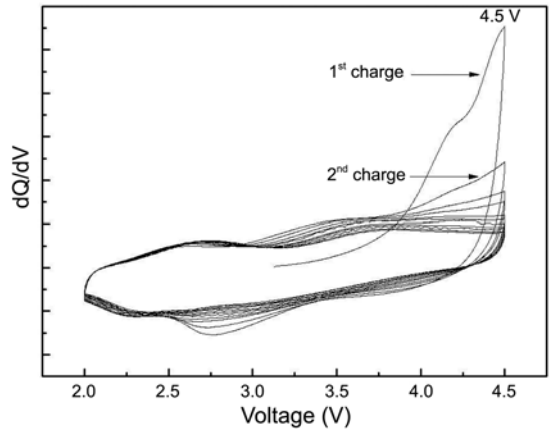

Figure 6. Cyclic voltammogram of $Li_2Mn_{0.5}Fe_{0.5}SiO_4$/C with a voltage range of 2.0~4.5 V at 0.1 mV/sec.

observed in the first cycle compare to the oxidation potential of Fe^{2+} to Fe^{3+}, we could presume that the reaction mechanism of this $Li_2Mn_{0.5}Fe_{0.5}SiO_4$/C nanocomposite is different with that of Li_2FeSiO_4, which the phenomenon can be attributed to a structure improvement process.[2,7] In the cycle performance as shown in Figure 5(b), the discharge capacity fades and saturated around 125 mAh/g and 63% of the initial discharge capacity was retained after 10 cycles. These monotonous smooth profile degradations behaviors in subsequent cycles indicated that amorphous electrode material degradation, which can be observed in another research.[8]

Figure 6 shows the dQ/dV curves of $Li_2Mn_{0.5}Fe_{0.5}SiO_4$/C. The $Li_2Mn_{0.5}Fe_{0.5}SiO_4$/C sample shows a pair of redox couple which is relatively broad, and the difference between the oxidation potential peak and reduction one is wide. According to the result, $Li_2Mn_{0.5}Fe_{0.5}SiO_4$/C exhibits larger hysteresis in the oxidation and reduction peaks and redox profile changes during cycles, which leading to its lower electrochemical reversibility and poorer cycle stability. This hysteresis phenomenon, which is of the thermodynamic origin and would always appear in many particle systems with non-homogeneous potential and phase, could be attributed to the structure amorphous phase of Li_2MnSiO_4 upon

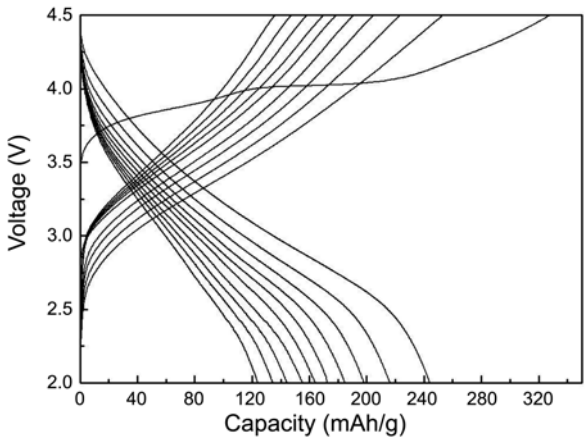

Figure 7. High temperature (55 °C) condition charge-discharge cycle performance of $Li_2Mn_{0.5}Fe_{0.5}SiO_4$/C.

first delithiation.[15]

High temperature (55 °C) charge-discharge profile is showed Figure 7. Voltage profile shows high charge-discharge capacity than room temperature. The effect of high temperature is improving ionic diffusivity and transfer activity and lower internal resistance. However high temperature cell test has disadvantages that poor cyclic ability since high temperature make faster degradation of structure. In the Figure 7 first discharge capacity is 244 mAh/g and after 10 cycle discharge capacity is 124 mAh/g (discharge capacity retention: 50%). Although high temperature test has high capacity, its low cyclic ability make problem for using Li-ion battery. In this cathode system, Mn-ion could influence by dissolution and migration to anode and deposition on the performances while high temperature condition at charge process.

Conclusions

We have demonstrated the synthesis of carbon coated $Li_2Mn_{0.5}Fe_{0.5}SiO_4/C$ nanocomposite by physical blending method. Crystallo-chemical studies of the orthosilicate $Li_2Mn_{0.5}Fe_{0.5}SiO_4/C$ has shown that this compound crystallizes in the orthorhombic structure ($Pmn2_1$ space group). $Li_2Mn_{0.5}Fe_{0.5}SiO_4/C$ sample exhibits well-formed crystallites of 30 nm size particles aggregate to ~300 nm in size. HR-TEM analysis showed that the sucrose made a 2-3 nm thick amorphous carbon coating layer on surface of the pristine $Li_2Mn_{0.5}Fe_{0.5}SiO_4$. The $Li_2Mn_{0.5}Fe_{0.5}SiO_4/C$ has a maximum discharge capacity of 200 mAh/g and show low cycling stability. Through the capacity of $Li_2Mn_{0.5}Fe_{0.5}SiO_4/C$, we can confirm that more than 1 mole Li ions per formula unit were reacted reversibly. In the first lithiation of $Li_2Mn_{0.5}Fe_{0.5}SiO_4/C$ nanocomposite, voltage profile change was observed due to amorphization. These structural instability directly connected with discharge capacity fading with increasing cycle number. High temperature test indicates high capacity performance however it shows rapid decline of cyclic performances might be attributed to the well-known Mn dissolution mechanism.

Acknowledgments. This work was supported by the Energy Efficiency & Resources of the Korea Institute of Energy Technology Evaluation and Planning (KETEP2008 EEL11P0800002009 and 20102010100090-11-2-200) grant funded by the Korea government Ministry of Knowledge Economy.

References

1. Dominko, R.; Bele, M.; Gaberscek, M.; Meden, A.; Remska, M.; Jamnik, J. *J. Electrochem. Commun.* **2006**, *8*, 217.
2. Nyten, A.; Abouimrane, A.; Armand, M.; Gustaffson, T.; Thomas, J. O. *J. Electrochem. Commun.* **2005**, *7*, 156.
3. Chebiam, R. V.; Prado, F.; Manthiram, A. *Chem. Mater.* **2001**, *12*, 2951.
4. Venkatraman, S.; Manthiram, A. *Chem. Mater.* **2002**, *14*, 3907.
5. Kim, J.; Noh, M.; Kim, J. H. *J. Electrochem. Soc.* **2005**, *152*, A1142.
6. Dominko, R. *J. Power Sources* **2008**, *184*, 462.
7. Dominko, R.; Conte, D. E.; Hanzel, D.; Gaberscek, M.; Jamnik, J. *J. Power Sources* **2008**, *178*, 842.
8. Belharouak, I.; Abouimrane, A.; Amine, K. *J. Phys. Chem.* **2009**, *113*, 20733.
9. Kokalj, A.; Dominko, R.; Mali, G.; Meden, A.; Gaberscek, M. *J. Jamnik, Chem. Mater.* **2007**, *19*, 3633.
10. Lyness, C.; Delobel, B.; Armstron, A. R.; Bruce, P. G. *Chem. Commun.* 2007; p 4890.
11. Nishimura, A. I.; Hayese, S.; Kanno, R.; Yashima, M.; Nakayama, N.; Yamada, A. *J. Am. Chem. Soc.* **2008**, *130*(40), 13212.
12. Muraliganth, T.; Stroukoff, K. R.; Manthiram, A. *Chem. Mater.* **2010**, *22*, 5754.
13. Gong, Z. L.; Li, Y. X.; He, G. N.; Yang, Y. *Electrochem. Solid State Lett.* **2008**, *11*(5), A60.
14. Deng, C.; Zhang, S.; Fu, B. L.; Yang, S. Y.; Ma, L. *Mater. Chem. Phys.* **2010**, *120*, 14.
15. Nyten, A.; Kamali, S.; Haggstrom, L.; Gustaffson, T.; Thomas, J. O. *Mater. Chem.* **2006**, *16*, 2266.